

## Article

# An Evaluation of the PV Integrated Dynamic Overhangs Based on Parametric Performance Design Method: A Case Study of a Student Apartment in China

Weifan Long <sup>1</sup>, Xiaofei Chen <sup>1,\*</sup>, Qingsong Ma <sup>1,2</sup> , Xindong Wei <sup>3</sup> and Qiao Xi <sup>1</sup>

<sup>1</sup> College of Architecture and Urban Planning, Qingdao University of Technology, Qingdao 266033, China; longweifan97@163.com (W.L.); maqingsong@qut.edu.cn (Q.M.); 19863763160@163.com (Q.X.)

<sup>2</sup> Innovation Institute for Sustainable Maritime Architecture Research and Technology (iSMART), Qingdao University of Technology, Qingdao 266033, China

<sup>3</sup> School of Environmental and Municipal Engineering, Jilin Jianzhu University, Changchun 130118, China; xindong33@hotmail.com

\* Correspondence: chenxiaofei@qut.edu.cn

**Abstract:** A photovoltaic shading device (PVSD) is a promising technology that can both generate electricity and provide shading to reduce indoor energy consumption. This paper aims to evaluate the performance of three PVSD design strategies in five Chinese cities by using a proposed all-in-one simulation program, according to the parametric performance design method. The program can be used to predict the energy consumption, power generation, and economic feasibility of different PVSD strategies. It was, firstly, calibrated through an actual experiment which was carried out in Qingdao and, secondly, used to simulate the energy consumption and generation of the three PVSD strategies in relation to the optimal angles and heights. Finally, the program was used to calculate the energy efficiency and economic feasibility of the three strategies. The findings indicated that the move-shade strategy of PVSD can provide the best energy-saving performance, followed by rotate-shade and fixed-shade strategies. Compared to the no-shade strategy, the reduction of the net energy use intensity by using the move-shade strategy was 31.80% in Shenzhen, 107.36% in Kunming, 48.37% in Wuhan, 61.79% in Qingdao, and 43.83% in Changchun. The payback periods of the three strategies ranged from 5 to 16 years when using the PVSD in China.

**Keywords:** PVSD; parametric design; performance evaluation; net energy use intensity (EUI); power generation



**Citation:** Long, W.; Chen, X.; Ma, Q.; Wei, X.; Xi, Q. An Evaluation of the PV Integrated Dynamic Overhangs Based on Parametric Performance Design Method: A Case Study of a Student Apartment in China. *Sustainability* **2022**, *14*, 7808. <https://doi.org/10.3390/su14137808>

Academic Editor: Antonio Caggiano

Received: 1 June 2022

Accepted: 23 June 2022

Published: 27 June 2022

**Publisher's Note:** MDPI stays neutral with regard to jurisdictional claims in published maps and institutional affiliations.



**Copyright:** © 2022 by the authors. Licensee MDPI, Basel, Switzerland. This article is an open access article distributed under the terms and conditions of the Creative Commons Attribution (CC BY) license (<https://creativecommons.org/licenses/by/4.0/>).

## 1. Introduction

Facing the pressure of increasing global environmental pollution, the application of renewable energy technologies can effectively reduce the consumption of fossil fuels and carbon emissions. China has pledged to reach carbon peaking by 2030, and carbon neutrality by 2060 [1]. In 2021, China has further issued the Action Plan for Carbon Peaking and aimed to achieve 20% and 25% of non-fossil energy consumption by 2025 and 2030, respectively [2]. With the implementation of various regional incentive policies, photovoltaic technology has been upgrading urban energy structures through continuous innovative development [3].

Photovoltaic (PV) technology can provide electricity for buildings, reduce their dependence on conventional grid power, and decrease urban carbon emissions and environmental pollution [4]. The integration of photovoltaic technology and architecture is developing in two directions: building-integrated photovoltaic (BIPV) and photovoltaic-integrated shading devices (PVSD) [5]. BIPV integrates photovoltaic components onto the facade and roof of buildings [6]. The integration of power-generation components and building envelope can create a simpler power-generation structure, higher photovoltaic efficiency, and a

more visually pleasant façade [7]. BIPV is widely used in energy-saving building design and green building reconstruction [8]. Photovoltaic-integrated shading devices (PVSD) combine shading components with photovoltaic panels. Compared with BIPV, PVSD is relatively simpler and cheaper. It is especially suitable for small-sized building renovation.

Due to the annual solar angle and radiation differences in various regions, the locations and modes of the optimal photovoltaic panel setting in each region are not the same [9]. In order to make efficient use of solar energy in different regions, single-axis tracking, dual-axis tracking [10], and concentrator photovoltaic (CPV) systems are being developed to maximize electricity generation [11,12]. There are also some studies that explored the possible ways to improve the energy efficiency of using PV panels. Agyekum et al. [13] found about a 12% improvement in energy efficiency and a 30% increase in power generation compared to the uncooled panels by using a cotton wick to cool the PV panels. They also discovered that the electricity efficiency of the PV panels can be improved by 6.8% and 5.85%, respectively, when using a heat sink (made up of aluminum fins and an ultrasonic humidifier) and a cooling system (made up of aluminum fins and paraffin wax) [14,15]. Similarly, PraveenKumar et al. [16] experimented with the aluminum sheets mounted PV panel module and found about a 4% increase in electricity efficiency and a 9.4% improvement in electricity generation, compared to conventional panels. However, PVSD, as a part of a building's external envelope structure, needs to consider its influence on building energy consumption, light environment, and indoor and outdoor visual effects under the condition of maintaining its own high-efficiency power generation [17]. Therefore, appropriate PVSD design requires multi-faceted optimization studies [18]. This should take the compatibility of PVSD with the local environment, the stability of PVSD technology, and the comfortability of users into consideration [19]. In order to maximize energy-use efficiency, it is necessary to consider the power-generation efficiency of PVSD, and, further, to propose economic feasibility schemes [20,21].

There are two ways of developing a dynamic PVSD strategy for buildings: (1) buildings adjusting themselves according to the changes of the external environment through rule-making [22]; and (2) finding the optimized results through the genetic algorithms or exhaustive simulation [23]. Svetozarevic et al. [24] developed a dynamic photovoltaic module that can cover 115% of net electricity demand by comprehensively assessing local power generation, shading, and daylighting. Optimization methods, such as genetic algorithms and machine learning, can locate parameters that support better performance of the dynamic systems [25]. Kirmat et al. [26] used genetic algorithms to calculate the total energy consumption and useful daylight illuminance (UDI) of the louver shading. They can achieve 14% energy savings, maintaining 50% UDI level. Taveres-Cachat et al. [18] employed a multi-objective optimization algorithm to explore the possible parameters of the static PVSD, and found that an optimized PVSD can improve the exploitation of solar energy.

Overall, existing studies on energy consumption of the dynamic PVSD strategy is rather limited. Among them, Ridha et al. [27] indicated that PVSD optimization is balanced by multiple objectives, which can further lead to different optimization results. For example, the tilt angles that generate the maximum amount of electricity can be different from the angles that produce the minimum amount of energy consumption. In the research of the optimal position of PVSD, Fouad et al. [28] pointed out that the optimal shading angle is close to the regional latitude value. Meysam [29] analyzed the impact of the suspended length of PVSD on the heating load of the building, and the impact of the tilt angle of PVSD on power generation. They selected a number of parameters to design a movable PVSD which is suitable for local climate and saves 290% energy, compared to the condition without the PVSD. Krarti [30] proposed a dynamic design strategy of PVSD according to monthly energy consumption and production with PV inclination angles at 0°, 45°, and 90°. They found that the dynamic PVSD can achieve net-zero energy consumption in a mild-climate region.

It is important to point out that finding optimal PVSD parameters, which can provide optimal energy performance in buildings, requires professional HVAC, computer science knowledge, and well-trained simulation techniques. However, without proper training, architects usually do not have the ability and knowledge to use energy performance simulation software, such as EnergyPlus, DoE-2, and TRNsys [31]. This undoubtedly increases the difficulties for architects to evaluate building performance through software simulation and further cause the absence of performance assessment in the design process [32]. The Ladybug and Honeybee plugins in the Grasshopper platform are developed from the EnergyPlus engine to evaluate the energy performance of buildings from various aspects. These plugins can simplify the simulation process and allow architects to evaluate building performance by using simplified settings and parameters, and further export data as visual graphics for analysis [33,34]. These plugins integrate parametric design and performance evaluation, and allow architects to understand scientifically how local climate and conditions can affect the performance of the architecture, and further propose flexible design schemes in the early design stage [35,36].

The main objective of this paper is to evaluate the energy performance of the application of three PVSD design strategies in five different Chinese cities by using a proposed all-in-one simulation program. The novelty of this study is to investigate the energy performance of the application of PVSD in student apartments in different climate zones in China by using the proposed parametric performance-design approach. This method integrates parametric design and performance evaluation, and it can assist architects to simplify the evaluation process and to optimize the various parameters to generate efficient PVSD design. In this paper, three PVSD design strategies are proposed and simulated in the application of a student apartment in five cities that are located in different climate zones. These strategies are analyzed and compared to show their advantages and differences, energy performances, and economic feasibilities. The findings indicate that the application of the PVSD proves its positive working efficiency in student apartments in China.

## 2. Methodology

### 2.1. PVSD Design Strategy

The application of PVSD in buildings is mainly used for shading, electricity generation, and insulation. Dynamic PVSD strategies are flexible to cope with the temperature changes throughout the year. In this research, it is designed to (a) provide shading and generate electricity when shading is needed; and (b) generate electricity at an optimal tilt angle and height when shading is not required. Theoretically, if a building façade has enough space to allow PVSD to move freely, dynamic PVSD could maximize the results of shading and electricity generation to improve energy efficiency. Based on the physical structure of the student apartment, the tilt angle of PVSD can change from  $0^\circ$  (horizontal) to  $90^\circ$  (vertical) at the interval of  $3^\circ$ . The moving distance of the dynamic PVSD is between  $-1.5$  m to  $1.5$  m at the interval of  $0.1$  m.

There are three PVSD design strategies: (1) static PVSD strategy (fixed-shade): employing exhaustive or genetic algorithms to select the optimal angle of the PVSD in a year according to net energy consumption (the difference between building energy consumption and the power generated by the PV), see Figure 1a; (2) rotation PVSD strategy (rotate-shade): employing exhaustive or genetic algorithms to select the optimal angle of the PVSD in each month according to the lowest net energy use intensity, see Figure 1b; (3) move and rotate PVSD strategy (move-shade): employing exhaustive or genetic algorithms to select the optimal moving distance and tilt angle of the PVSD in each month according to the lowest net energy use intensity, see Figure 1c.

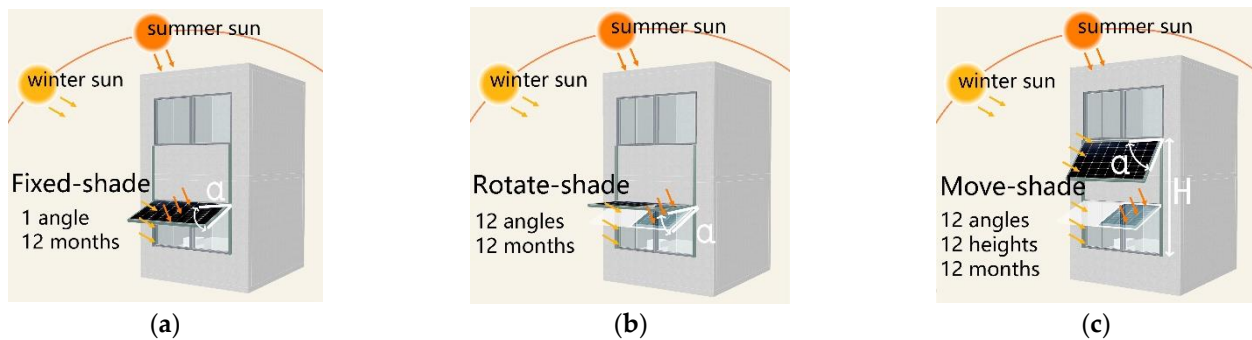


**Figure 1.** Three strategies for using PVSD in winter and summer: (a) fixed-shade; (b) rotate-shade; and (c) move-shade.

## 2.2. Simulation Workflow

Figure 2 shows the parametric performance design methodology and the flowchart of PVSD performance evaluation. As indicated in Figure 2a, given certain objectives, designers can input various parameters and rules to allow the computer to generate and assess a number of design possibilities through genetic or exhaustive algorithms. Designers can choose the optimal design solutions from computer calculated and filtered outcomes. Figure 2b is a flowchart that illustrates the design generation process in more detail. The fixed parameters (including building geometry, building construction, HVAC system, loads and schedules, and meteorological data) and dynamic parameters (including the moving height and tilt angle of PVSD) are, firstly, set to create the zone geometry and assign properties for the zone. Then the generated PVSD solutions are evaluated according to if the targets (minimum annual net energy consumption and shortest payback period) can be met. Finally, designers can select the optimal solutions from the output results.

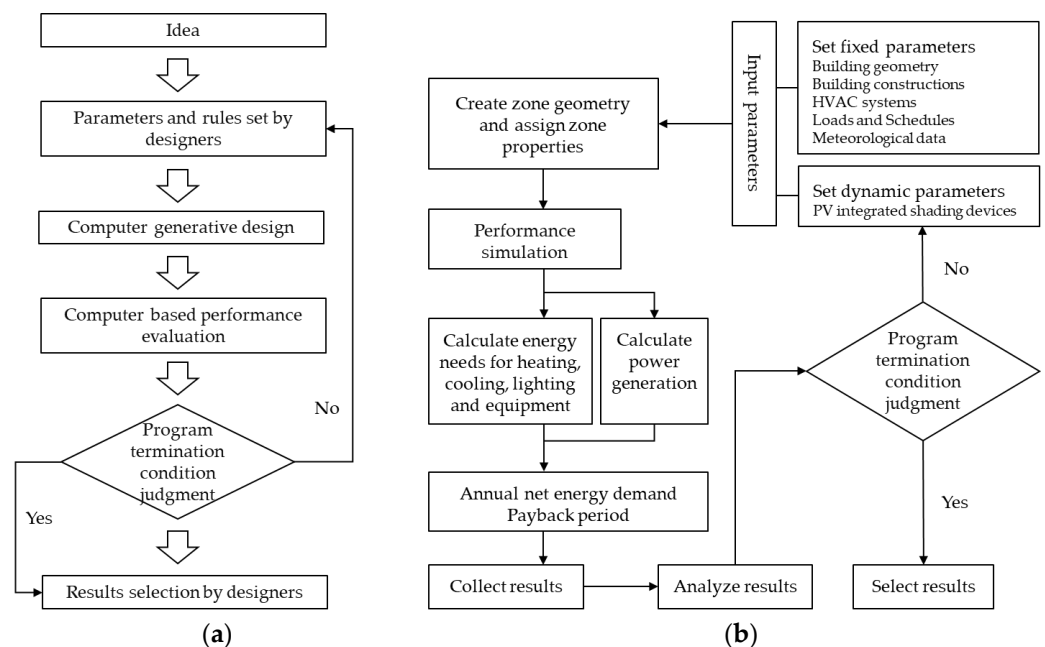


**Figure 2.** Research methodology and workflow. (a) Parametric performance design methodology; (b) PVSD performance evaluation flowchart.

In order to simplify the simulation process of the performance of PVSD, Ladybug 0.0.69 and Honeybee 0.0.66 are used to build the simulation program in the Grasshopper platform as indicated in Figure 3, which illustrates the overall workflow. The model script includes three main sections: input parameters, performance evaluation, and objective optimization. In this research, the HVAC system adopts the ideal air load to quantify buildings' heating



and cooling energy consumptions, which means the coefficient of performance (COP) of the HVAC system is equal to 1 [37]. The room temperature should be maintained between 18 °C and 26 °C, according to China's regulations [38]. The photovoltaic battery is a TD7G66M132 half-cell with 485 w electric power and 20% photoelectric conversion efficiency [39]. The transfer efficiency between DC and AC is 90%. In order to evaluate the impact of different design strategies on PVSD, the following three criteria are adopted in this study: (1) energy use intensity (EUI): assessing the overall energy consumption of a building; (2) photovoltaic power generation (PPG): assessing the power generation of the photovoltaic shading system; and (3) net energy use intensity (net EUI): net EUI = EUI – PPG, assessing the energy saving performance of the photovoltaic shading system.

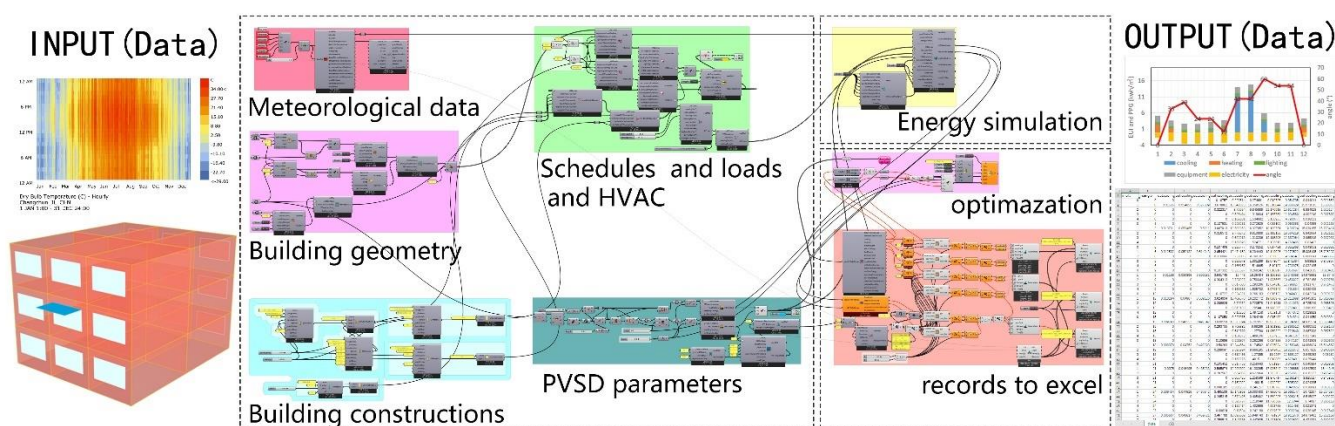


**Figure 3.** Visualization of the simulation program workflow in the Grasshopper platform.

### 2.3. Experiment

The experiment room was selected in a student apartment in Qingdao, China. The experimental room was located in the middle of the apartment, and the room size was: 3.6 m × 6.3 m × 3 m. The window size of the room was: 2.6 m × 1.5 m. The spacings on the two sides of these windows were small, and the upper and lower spacings were large. There was no obstruction to the facade of the building. The building wall construction is 300 mm concrete, with 1 mm plastering on both sides. Table 1 shows the related building parameters. The TESTO 174 h meters were installed at the height of 0.75 m in the apartment for measurement, and they were used to measure the room temperature with the range between −20 and 70 °C and an accuracy of ±0.5 °C. As shown in Figure 4, measurement points A and B in the case study room are clearly indicated.

**Table 1.** Building parameters.

Parameter Name	Quantity
Total floor area	22.68 m <sup>2</sup>
Window area	3.9 m <sup>2</sup>
Infiltration rate per area façade	0.0006 m <sup>3</sup> /s·m <sup>2</sup>
Number of people	2
Lighting load	3.17 W/m <sup>2</sup>
Equipment load	3.88 W/m <sup>2</sup>
Wall construction u-value	2.2 w/m <sup>2</sup> ·K
Window construction u-value	5.5 w/m <sup>2</sup> ·K

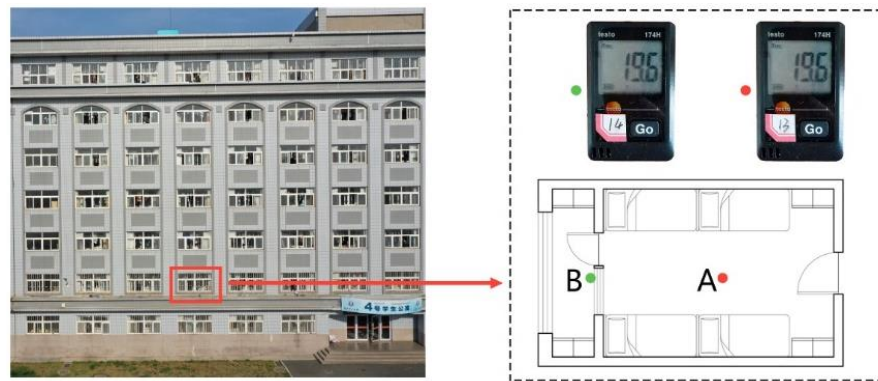


**Figure 4.** The student apartment (left) and the experiment room (right). The temperature meters were installed at measurement points A and B.

### 3. Results

#### 3.1. Model Validation

In the simulation program, the student apartment was simplified into 18 rooms, as shown in Figure 3. Figure 5 indicates the indoor and outdoor temperatures per hour in the experiment and simulation in April 2022. The simulation result shows a similar trend as the experimental result. By using the mean absolute error (MAE), as indicated in (1):

$$MAE = \frac{1}{n} \sum_{i=1}^n |f_i - y_i| \quad (1)$$

where  $f_i$  is the simulation value, and  $y_i$  is the measurement value.

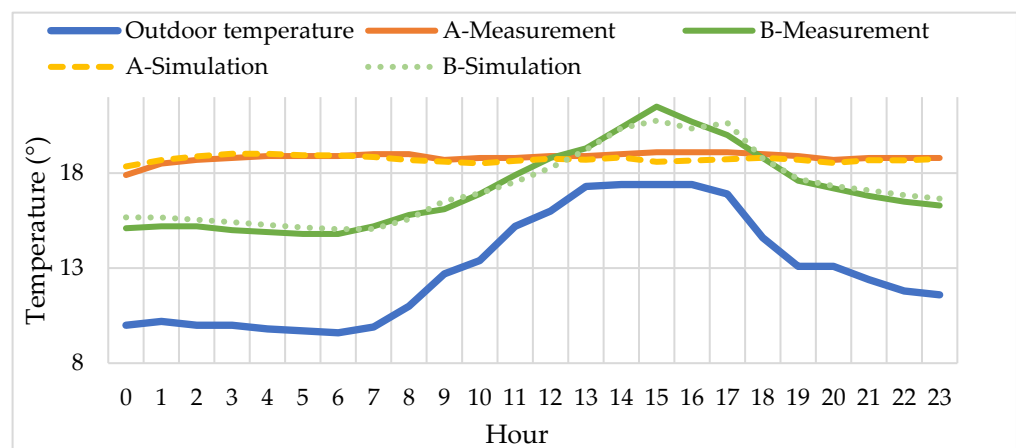


**Figure 5.** Hourly indoor and outdoor air temperature of the experimental and simulation.

The average absolute errors of the results of the measurement point A and B in the experiment and the simulation were 0.2 °C and 0.3 °C, respectively. In the subsequent studies, the simulation program for the PVSD evaluation as discussed in Section 2.2 was used to analyze the energy performance of PVSD in the five case-study cities.

#### 3.2. Power Generation in Five Cities

In order to compare the impact of the application of PVSD in different climate zones, five cities in China were selected for analysis. Meteorological data were from the One Building website [40]. In Figure 6a, the five case study cities are Shenzhen, Kunming, Wuhan, Qingdao, and Changchun. They are located in the region with increasing latitude, covering 21.3° geographically from north to south. The five cities are located in hot summer and warm winter, moderate climate, hot summer and cold winter, cold, and severe cold

climate zones, respectively [41]. Figure 6b shows the amount of electricity generated by the PVSD, which was installed on the south-facing façade of the student apartment in the five cities.

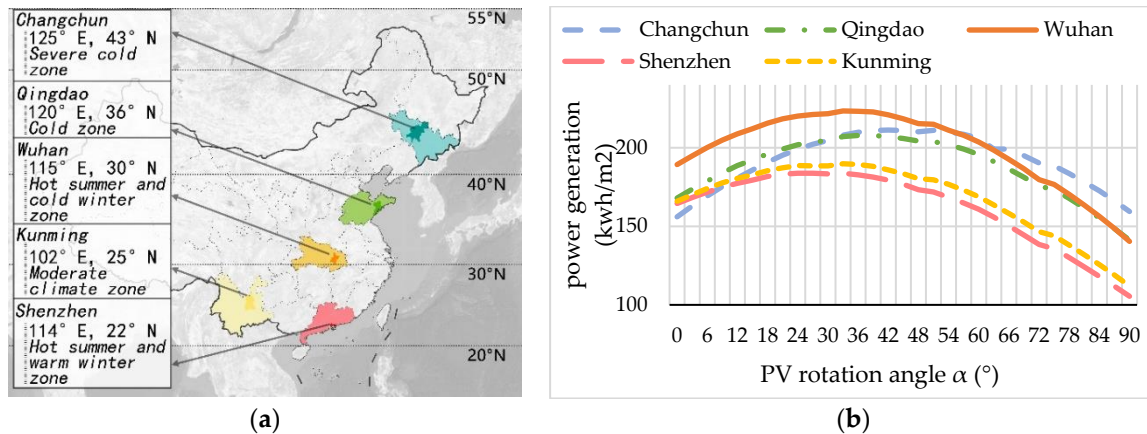


**Figure 6.** The relationship between the tilt angle of the PVSD and power generation in the five case-study cities. (a) city location and climate zone; (b) the amount of electricity generated by the PVSD in a year.

With the increasing latitudes of the cities, the tilt angles of the PVSD also increased. The optimal tilt angles to generate the maximum amount of electricity for Shenzhen, Kunming, Wuhan, Qingdao, and Changchun were 27°, 33°, 33°, 39°, and 42°, respectively. This shows that with the increasing urban latitude, photovoltaic technology requires greater inclination to achieve greater power generation. The peak values of the power generation of the PVSD in Wuhan, Changchun, Qingdao, Kunming, and Shenzhen are 233 kWh/m<sup>2</sup>, 211 kWh/m<sup>2</sup>, 207 kWh/m<sup>2</sup>, 190 kWh/m<sup>2</sup>, and 184 kWh/m<sup>2</sup>, respectively. The latitude of Wuhan is in the middle of the five cities, showing the highest amount of power generation. Cities with a latitude of 30° or more can generate a greater amount of power than the PVSD in the equatorial area. A reason for this result is related to the solar movement trajectory in different cities.

### 3.3. Results of the PVSD Strategies

This section analyzes the results of the three PVSD strategies in five selected cities. It demonstrates the effect of the PVSD three strategies in a student apartment, as discussed in Section 2.1. The impact of the PVSD on buildings is explained from two aspects: (1) the impact of PVSD on cooling and heating loads; and (2) ratio of power generation to energy consumption.

#### 3.3.1. In Shenzhen

Shenzhen is located in the hot summer and warm winter climate zone. The average temperature in January is 16 °C, and the average temperature in July is 30 °C. Figure 7 shows the monthly energy consumption of the PVSD in Shenzhen by using different design strategies. When no shading was applied, cooling was required throughout the year, but heating is not needed for this city as indicated in Figure 7a. The energy consumption of one year is about 147 kWh/m<sup>2</sup>. The cooling energy consumption accounts for 78.54% of the annual energy consumption, and the cooling energy consumption from May to October accounts for 90% of the annual cooling energy consumption. The cooling load was the highest (20 kWh/m<sup>2</sup>) in August.

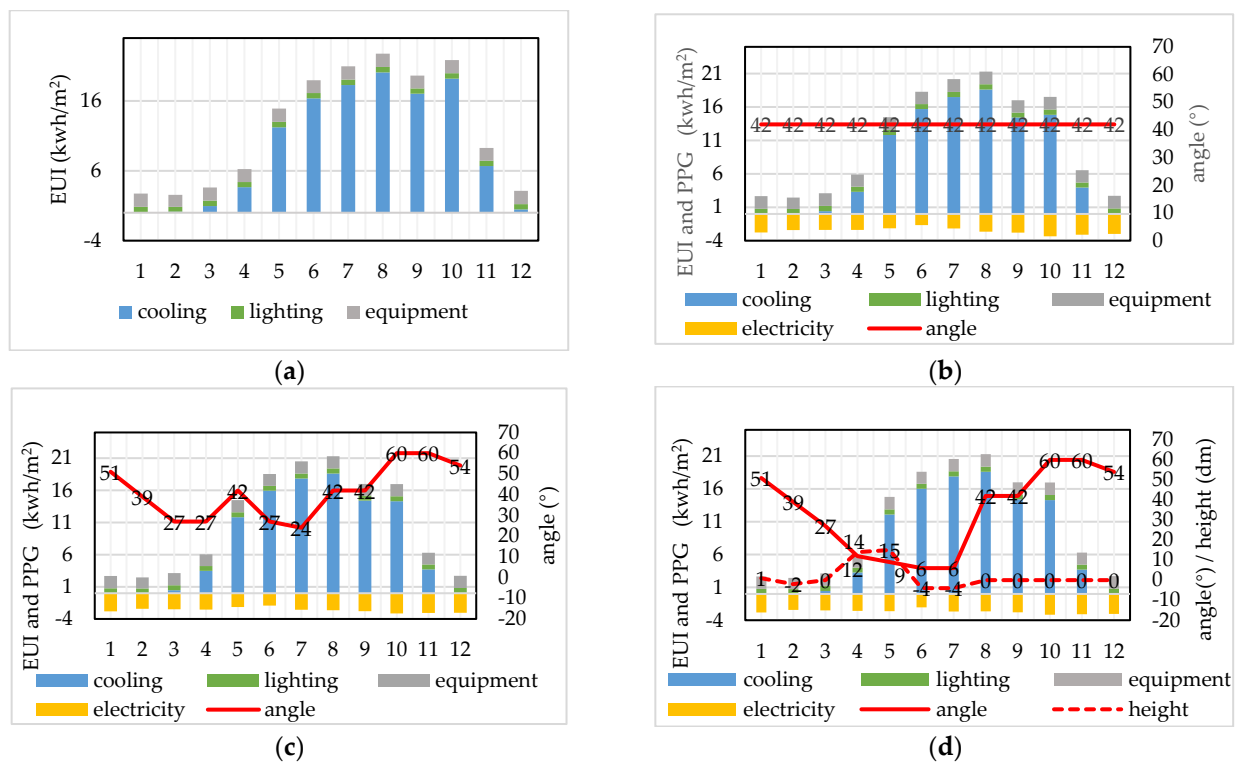


**Figure 7.** The energy consumption intensity (EUI) and photovoltaic power generation (PPG) by using different PVSD strategies in Shenzhen: (a) no-shade; (b) fixed-shade; (c) rotate-shade; and (d) move-shade.

By using the fixed-shade strategy, the optimal tilt angle for the PVSD was 42° as shown in Figure 7b. At this angle, the annual energy consumption is 132.12 kWh/m<sup>2</sup>. The highest cooling load reduction was 4.3 kWh/m<sup>2</sup> in October, and the total cooling load of the year was reduced by 12.6%, compared to the condition as shown in Figure 7a. The highest cooling load was about 18.6 kWh/m<sup>2</sup> in August. The total amount of electricity generated by the PVSD was 30.84 kWh/m<sup>2</sup>, which can occupy about 23.34% of the total energy consumption of a year. The lowest amount of power generation was in June (1.67 kWh/m<sup>2</sup>), while the highest was found in October (3.35 kWh/m<sup>2</sup>).

By using the rotate-shade strategy, the optimal angles of the PVSD from January to December were 51°, 39°, 27°, 27°, 42°, 27°, 24°, 42°, 42°, 60°, 60°, and 54°, respectively, as indicated in Figure 7c. The annual energy consumption is 132.13 kWh/m<sup>2</sup>. The cooling load was reduced by 12.6%, compared to the condition as shown in Figure 7a. The highest reduction of cooling load (4.8 kWh/m<sup>2</sup>) was in October. The annual PV generated electricity was 31.62 kWh/m<sup>2</sup>, which took up about 23.93% of the total energy consumption. The lowest amount of PV generated electricity was found in June (1.93 kWh/m<sup>2</sup>), and the highest was in October (3.15 kWh/m<sup>2</sup>).

By using the move-shade strategy, the PVSD was set to find the lowest net energy consumption by changing the tilt angle and height of PVSD. The optimal angles from January to December were 51°, 39°, 27°, 12°, 9°, 6°, 6°, 42°, 42°, 60°, 60°, and 54°, and the optimal heights were 0.1, -0.2, 0, 1.4, 1.5, -0.4, -0.4, 0, 0, 0, 0, and 0 m, respectively, as shown in Figure 7d. This means that the height of the PVSD should not be changed from August to December, when the PVSD was set to the optimal angle of those months. The annual energy consumption is 132.39 kWh/m<sup>2</sup>. The cooling load was reduced by 12.37%, compared to the condition as shown in Figure 7a. The total amount of electricity generated by the PVSD was 32.39 kWh/m<sup>2</sup>, which took 24.46% of the total energy consumption in a year. Again, the lowest amount of electricity was produced in June (2.05 kWh/m<sup>2</sup>), while the highest was in October (3.15 kWh/m<sup>2</sup>).



### 3.3.2. In Kunming

Kunming is located in the moderate climate zone. The average temperature in January is 10 °C, and the average temperature in July is 20 °C. Figure 8 shows the monthly energy consumption in Kunming by using different PVSD design strategies. The demand for heating and cooling throughout the year was weak as shown in Figure 8a. When there was no shading, the heating load was only found in January. The cooling load appeared from April to October and took 67% of the total cooling load of the year. The total energy consumption was 32.62 kWh/m<sup>2</sup>. The heating and cooling load were only accounted for 3.53% of the total energy consumption. Most energy was used to support lighting and equipment.

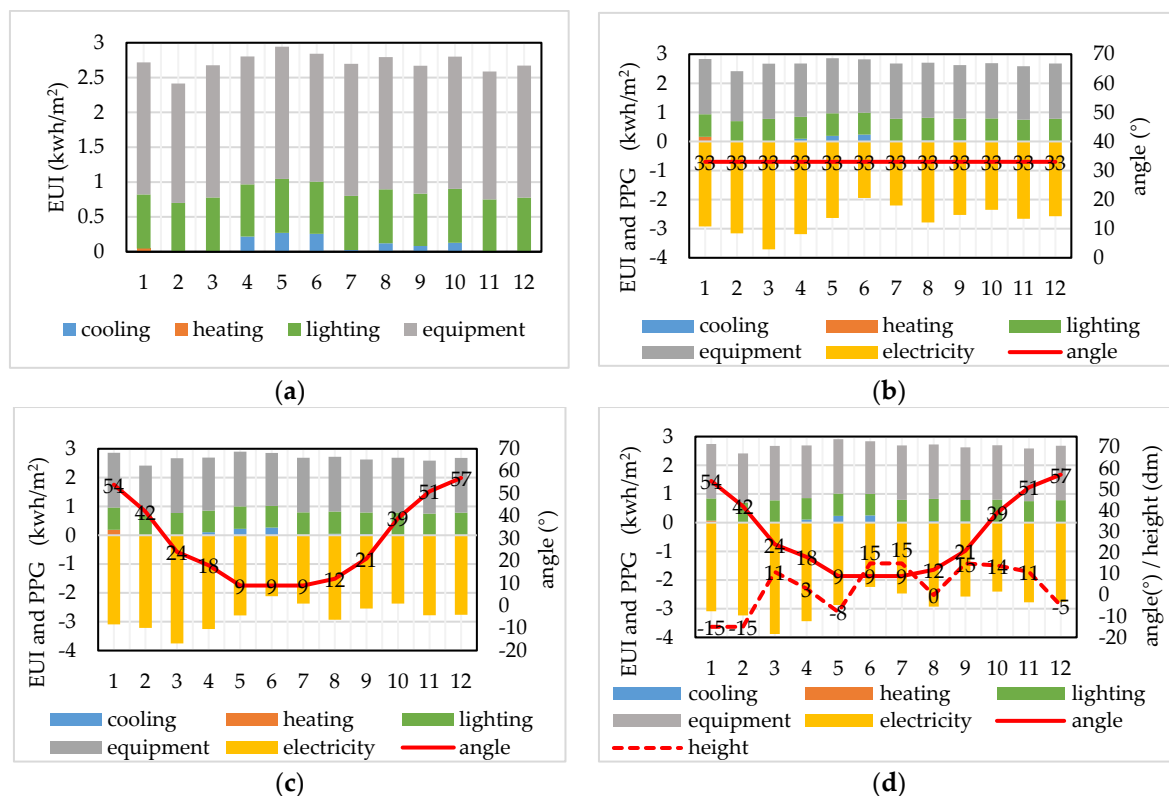


**Figure 8.** The energy consumption intensity (EUI) and photovoltaic power generation (PPG) by using different PVSD strategies in Kunming: (a) no-shade; (b) fixed-shade; (c) rotate-shade; and (d) move-shade.

When the fixed-shade strategy was applied as indicated in Figure 8b, 33° was found to be the optimal angle of the year for using the PVSD. At this optimal angle, the annual energy consumption is 32.26 kWh/m<sup>2</sup>. The total energy consumption was reduced, although the cooling load decreased, and the heating load increased. The total amount of electricity produced by the PVSD was 32.64 kWh/m<sup>2</sup>, which accounted for 101.18% of the total energy consumption of the year. The lowest amount of power generation was in June (1.94 kWh/m<sup>2</sup>), while the highest was found in March (3.71 kWh/m<sup>2</sup>).

By using the rotate-shade strategy, the optimal angles of the PVSD from January to December were 54°, 42°, 24°, 18°, 9°, 9°, 9°, 12°, 21°, 39°, 51°, and 57°, respectively, as indicated in Figure 8c. The annual energy consumption is 32.39 kWh/m<sup>2</sup>. The cooling load decreased, and the heating load increased. The annual PV generated electricity was 33.96 kWh/m<sup>2</sup>, which took up to 104.86% of the total energy consumption. The lowest amount of electricity produced by the PVSD was found in June (2.12 kWh/m<sup>2</sup>), and the highest was in March (3.75 kWh/m<sup>2</sup>).

When applying the move-shade strategy, the optimal angle of each month was the same as the one in Figure 8c. The optimal heights from January to December were  $-1.5$ ,  $-1.5$ ,  $1.1$ ,  $0.3$ ,  $-0.8$ ,  $1.5$ ,  $1.5$ ,  $0$ ,  $1.5$ ,  $1.4$ ,  $1.1$ , and  $-0.5$  m, respectively, and the height of the PVSD should not be changed in August. This is because the heating and cooling loads were extremely low in Kunming. The net energy consumption was mainly reduced through photovoltaic power generation. The annual PV generated electricity was  $34.67 \text{ kWh/m}^2$ , which took up to 107.46% of the total energy consumption. Again, the total amount of electricity generated by the PVSD was the lowest in June ( $2.24 \text{ kWh/m}^2$ ) and highest in March ( $3.88 \text{ kWh/m}^2$ ). This phenomenon implies that due to the local climate of Kunming, it can achieve nearly zero energy consumption through installing the PVSD.

### 3.3.3. In Wuhan

Wuhan is located in the hot summer and cold winter climate zone. The average temperature in January is  $4 \text{ }^\circ\text{C}$ , and the average temperature in July is  $30 \text{ }^\circ\text{C}$ . Figure 9 illustrates the monthly energy consumption in Wuhan by using different PVSD design strategies. With no shading system applied, the cooling load mainly occurred between April and October as shown in Figure 9a. The cooling load was the highest in July, reaching  $23 \text{ kWh/m}^2$ . The heating load mainly occurred between December and March, and the highest heating load was  $0.60 \text{ kWh/m}^2$  in January. The total energy consumption throughout the year was  $103.53 \text{ kWh/m}^2$ . It is important to point out that the simulation room was located in the middle of eight rooms with only one side facing south and contacting the outdoor environment. Thus, the energy exchange between the surrounding rooms and the simulated room was less than the energy exchange between the surrounding rooms and the outdoor environment. As a result, there was less heat loss in the simulated room than the other rooms, so the heating load was relatively low.

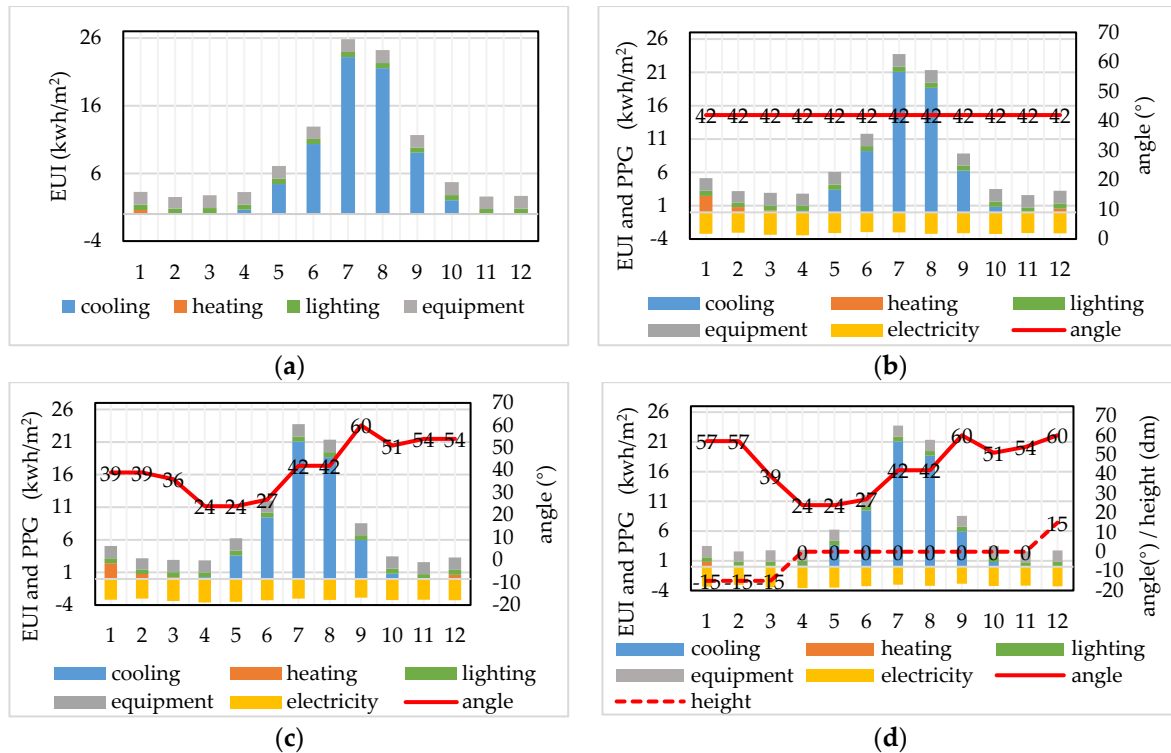


**Figure 9.** The energy consumption intensity (EUI) and photovoltaic power generation (PPG) by using different PVSD strategies in Wuhan: (a) no-shade; (b) fixed-shade; (c) rotate-shade; and (d) move-shade.

When applying fixed-shade strategy, the optimal tilt angle of the PVSD was  $42^\circ$ , as indicated in Figure 9b. At this angle, the total energy consumption throughout the year

was 95.19 kWh/m<sup>2</sup>. The total energy consumption was reduced, the total cooling load was decreased by 12 kWh/m<sup>2</sup> and the heating load was increased by 3 kWh/m<sup>2</sup>. The total amount of electricity generated in a year was 37.99 kWh/m<sup>2</sup>, which accounted for 39.90% of the total energy consumption. The lowest amount of electricity generated by the PVSD was in June (2.94 kWh/m<sup>2</sup>), and the highest (3.44 kWh/m<sup>2</sup>) was in April.

With the rotate-shade strategy, the optimal angles of the PVSD from January to December were 39°, 39°, 36°, 24°, 24°, 27°, 42°, 42°, 60°, 51°, 54°, and 54°, respectively, as indicated in Figure 9c. Similar to the results in Kunming, the cooling load decreased, while the heating load increased. The total energy consumption throughout the year was 95.32 kWh/m<sup>2</sup>. The annual PVSD generated electricity was 38.73 kWh/m<sup>2</sup>, which took up to 40.64% of the total energy consumption. The lowest amount of electricity produced by the PVSD was found in September (2.86 kWh/m<sup>2</sup>), and the highest was in April (3.60 kWh/m<sup>2</sup>).

By using the move-shade strategy, the optimal angles of the PVSD from January to December were 57°, 57°, 39°, 24°, 24°, 27°, 42°, 42°, 60°, 51°, 54°, and 60°, and the optimal heights were −1.5, −1.5, −1.5, 0, 0, 0, 0, 0, 0, 0, and 1.5 m, respectively. While keeping the optimal angle in each month, the height of the PVSD mostly remained unchanged throughout the year. The results as shown in Figure 9d indicates that the total cooling load of the year can be reduced by changing the height of the PVSD. The result was similar but slightly lower in comparison to the fixed-shade and rotate-shade strategies. The heating load increased, but the magnitude of the increase was low. The total energy consumption throughout the year was 92.43 kWh/m<sup>2</sup>. The total amount of PVSD generated electricity was 40.23 kWh/m<sup>2</sup>, which took 42.17% of the total energy consumption of the year. The lowest amount of electricity generated by the PVSD was in February (3.05 kWh/m<sup>2</sup>), and the highest (3.60 kWh/m<sup>2</sup>) was in April.

### 3.3.4. In Qingdao

Qingdao is located in the cold climate zone. The average temperature in January is 0 °C, and the average temperature in July is 26 °C. Figure 10 illustrates the monthly energy consumption in Qingdao by using the different PVSD design strategies. With no shading system applied, the cooling load was found between May and October as shown in Figure 10a. The highest cooling load was 14 kWh/m<sup>2</sup> in August, and the cooling load in July and August accounted for up to 75% of the total cooling load of the year. The heating load mainly concentrated between November and February, and the highest heating load was 69.73 kWh/m<sup>2</sup> in January. The total energy consumption throughout the year was 69.73 kWh/m<sup>2</sup>.

When applying the fixed-shade strategy, the optimal tilt angle of the PVSD throughout the year was 36° as indicated in Figure 10b. At this angle, the total energy consumption was increased, although the total cooling load was decreased by 6.45 kWh/m<sup>2</sup> and the heating load was increased by 7.14 kWh/m<sup>2</sup>. The total energy consumption throughout the year was 70.42 kWh/m<sup>2</sup>. The total amount of electricity generated by the PVSD in a year was 35.73 kWh/m<sup>2</sup>, and it accounted for 50.74% of the total energy consumption. The lowest amount of electricity generated by the PVSD was in November (2.35 kWh/m<sup>2</sup>), and the highest (3.60 kWh/m<sup>2</sup>) was in March.

With the rotate-shade strategy, the optimal angles of the PVSD from January to December were 0°, 33°, 39°, 24°, 24°, 12°, 42°, 42°, 60°, 54°, 54°, and 0°, respectively, as indicated in Figure 10c. The tilt angles of the PVSD in December and January are both 0°, it means that there was no need to provide shading, and the power generation cannot make up for the energy consumed by the PVSD in the two months. The total cooling load of the year was reduced by 6.95 kWh/m<sup>2</sup>, the heating load was increased by 3.57 kWh/m<sup>2</sup>. The total energy consumption throughout the year was 70.42 kWh/m<sup>2</sup>. The total amount of electricity generated by the PVSD was 33.71 kWh/m<sup>2</sup>, which took up to 50.81% of the energy consumption of the year. The lowest amount of electricity generated by the PVSD was in December (1.36 kWh/m<sup>2</sup>), and the highest (3.70 kWh/m<sup>2</sup>) was in May.

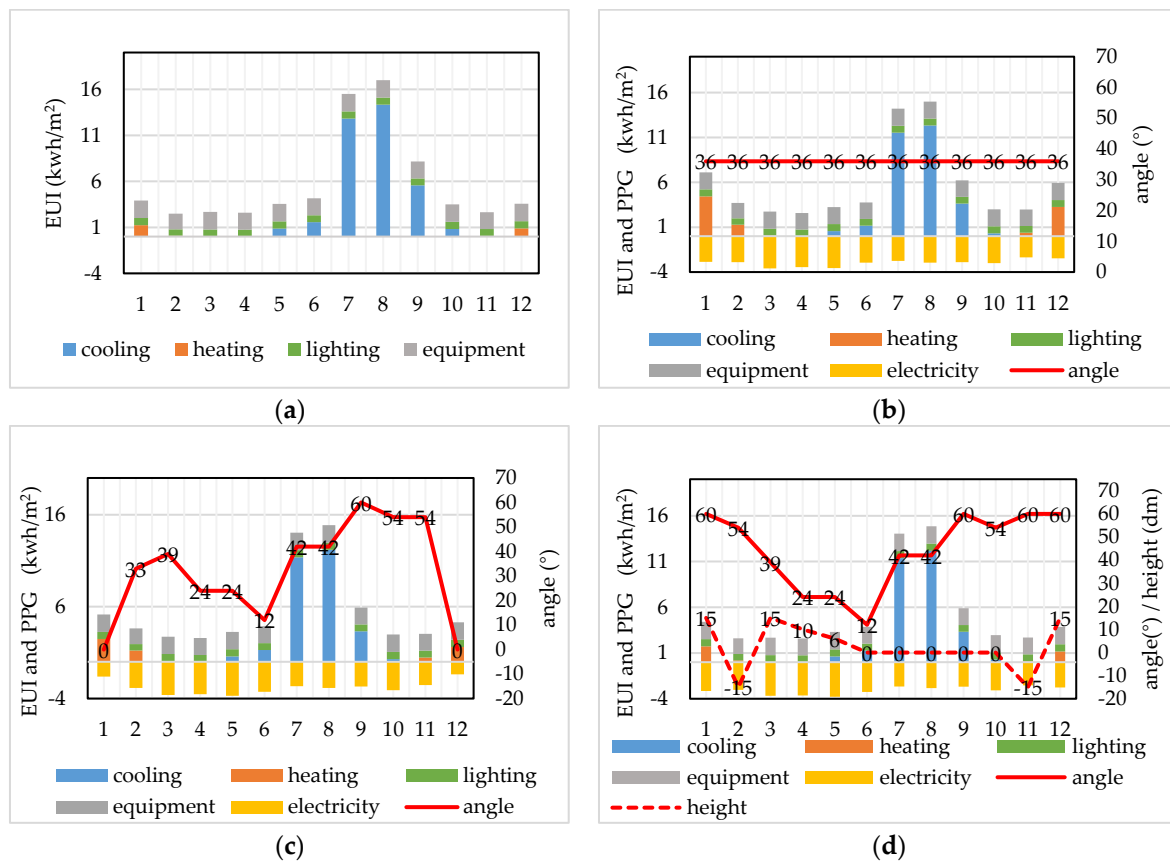


**Figure 10.** The energy consumption intensity (EUI) and photovoltaic power generation (PPG) by using different PVSD strategies in Qingdao: (a) no-shade; (b) fixed-shade; (c) rotate-shade; and (d) move-shade.

By using the move-shade strategy, the optimal angles of the PVSD from January to December were  $60^\circ$ ,  $54^\circ$ ,  $39^\circ$ ,  $24^\circ$ ,  $24^\circ$ ,  $12^\circ$ ,  $42^\circ$ ,  $42^\circ$ ,  $60^\circ$ ,  $54^\circ$ ,  $60^\circ$ , and  $60^\circ$ , and the optimal heights were 1.5,  $-1.5$ , 1.5, 1, 0.6, 0, 0, 0, 0,  $-1.5$ , and 1.5 m, respectively. While keeping the optimal angle, the height of the PVSD remained unchanged from June to October. The results as shown in Figure 10d indicates that the total cooling load of the year can be reduced by changing the height of the PVSD. The total cooling load can be reduced by  $6.91 \text{ kWh/m}^2$  despite the heating load being increased by  $0.93 \text{ kWh/m}^2$ . The total energy consumption throughout the year was  $66.35 \text{ kWh/m}^2$ . The total amount of PV generated electricity was  $37.11 \text{ kWh/m}^2$ , which took 58.21% of the total energy consumption of the year. The lowest amount of electricity generated by the PVSD was in November ( $2.54 \text{ kWh/m}^2$ ), and the highest ( $3.80 \text{ kWh/m}^2$ ) was in May.

### 3.3.5. In Changchun

Changchun is located in severe cold climate zone. The average temperature in January is  $-14^\circ\text{C}$ , and the average temperature in July is  $24^\circ\text{C}$ . Figure 11 illustrates the monthly energy consumption in Changchun by using different PVSD design strategies. Without any shading, cooling and heating were both needed, and the energy used for heating was greater than the energy used for cooling. The total energy consumption was  $86.20 \text{ kWh/m}^2$ . The cooling load of the PVSD mainly occurred between May and September, accounting for 17.20% of the annual energy consumption. The cooling load in July and August took up to 82% of the total energy consumption of one year, as shown in Figure 11a. The heating load was found between November and April, and the heating load was the highest ( $12.73 \text{ kWh/m}^2$ ) in January.

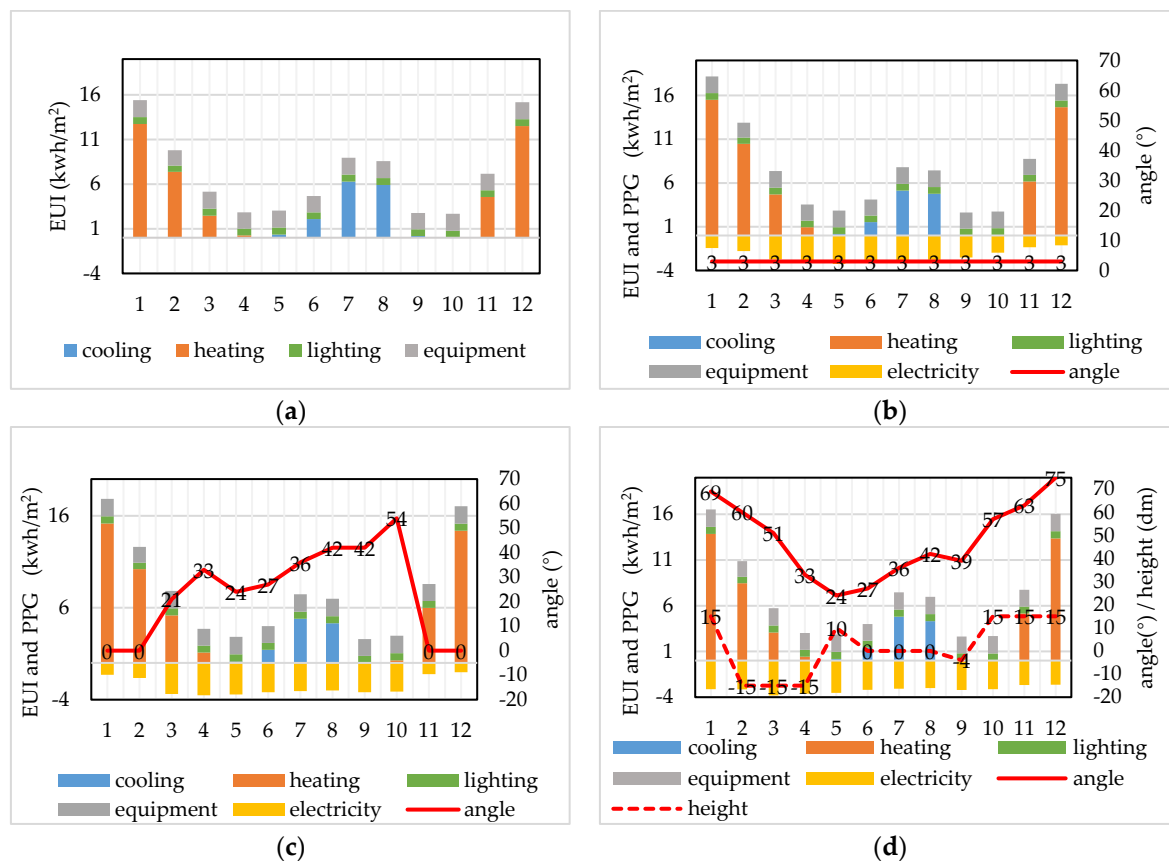


**Figure 11.** The energy consumption intensity (EUI) and photovoltaic power generation (PPG) by using different PVSD strategies in Changchun: (a) no-shade; (b) fixed-shade; (c) rotate-shade; and (d) move-shade.

When applying the fixed-shade strategy, the optimal tilt angle of the PVSD was  $3^\circ$  as indicated in Figure 11b. At this angle, the total cooling load was decreased by  $3.20 \text{ kWh/m}^2$ , but the heating load was increased by  $12.58 \text{ kWh/m}^2$ , and the total energy consumption was still increased. The total energy consumption was  $95.57 \text{ kWh/m}^2$ . The total amount of electricity generated by the PVSD in a year was  $28.02 \text{ kWh/m}^2$ , and it accounted for 29.31% of the total energy consumption. The lowest amount of electricity generated by the PVSD was in December ( $1.13 \text{ kWh/m}^2$ ), and the highest ( $3.24 \text{ kWh/m}^2$ ) was in May.

By using the rotate-shade strategy, the optimal tilt angles of the PVSD from January to December were  $0^\circ$ ,  $0^\circ$ ,  $21^\circ$ ,  $33^\circ$ ,  $24^\circ$ ,  $27^\circ$ ,  $36^\circ$ ,  $42^\circ$ ,  $42^\circ$ ,  $54^\circ$ ,  $0^\circ$ , and  $0^\circ$ , respectively, as indicated in Figure 11c. The tilt angles of the PVSD from November to February were all  $0^\circ$ , which means that there was no need to provide shading, and the power generation cannot make up for the energy consumed by the PVSD system in the four months. The total energy consumption of the year was increased, while the total cooling load of the year was reduced by  $4.13 \text{ kWh/m}^2$ , and the heating load was increased by  $12.39 \text{ kWh/m}^2$ . The total energy consumption was  $94.46 \text{ kWh/m}^2$ . The total amount of electricity generated by the PVSD was  $31.08 \text{ kWh/m}^2$ , which accounted for 32.90% of the energy consumption of the year. The lowest amount of electricity generated by the PVSD was in December ( $1.01 \text{ kWh/m}^2$ ), and the highest ( $3.53 \text{ kWh/m}^2$ ) was in April.

With the move-shade strategy, the optimal tilt angles of the PVSD from January to December were  $69^\circ$ ,  $60^\circ$ ,  $51^\circ$ ,  $33^\circ$ ,  $24^\circ$ ,  $27^\circ$ ,  $36^\circ$ ,  $42^\circ$ ,  $39^\circ$ ,  $57^\circ$ ,  $63^\circ$ , and  $75^\circ$ , and the optimal heights were 1.5,  $-1.5$ ,  $-1.5$ ,  $-1.5$ , 1, 0, 0, 0,  $-0.4$ , 1.5, 1.5, and 1.5 m, respectively. The height of the PVSD was not changed from June to August when it was kept at the optimal tilt angle in each month. The results as shown in Figure 11d indicate that the total cooling load of the year was even slightly increased by changing the height of the PVSD, while the total cooling load was reduced by  $4.07 \text{ kWh/m}^2$ , and the heating load was increased



by 4.42 kWh/m<sup>2</sup>. The total energy consumption was 86.54 kWh/m<sup>2</sup>. The total amount of PV generated electricity was 38.12 kWh/m<sup>2</sup>, which took 44.05% of the total energy consumption of the year. The lowest amount of electricity generated by the PVSD was in December (2.62 kWh/m<sup>2</sup>), and the highest (3.80 kWh/m<sup>2</sup>) was in March.

### 3.4. Energy Efficiency and Economic Feasibility

Figure 12 shows the results of the net EUI by using the three PVSD strategies in comparison to the no-shade condition in the five cities. In general, the move-shade strategy performed the best in all the five cities in terms of energy saving, and it was followed by rotate-shade and fixed-shade strategies. Among them, Kunming achieved net-zero energy consumption. Comparing to the no-shade strategy, the reduction of the net EUI by using the move-shade strategy was 31.80% in Shenzhen, 48.37% in Wuhan, 61.79% in Qingdao, and 43.83% in Changchun. Comparing the fixed-shade strategy, the reduction of net EUI by using the move-shade strategy was 1.26% in Shenzhen, 6.57% in Wuhan, 23.21% in Qingdao, and 28.33% in Changchun. Comparing the rotate-shade strategy, the reduction of net EUI by using the move-shade strategy was 0.51% in Shenzhen, 5.55% in Wuhan, 18.36% in Qingdao, and 23.60% in Changchun. The difference between the net EUI values by using the three PVSD strategies was the smallest in Shenzhen, and the largest in Changchun. The results indicate that the effects of various strategies in different regions are disparate, and different strategies should be applied case by case.

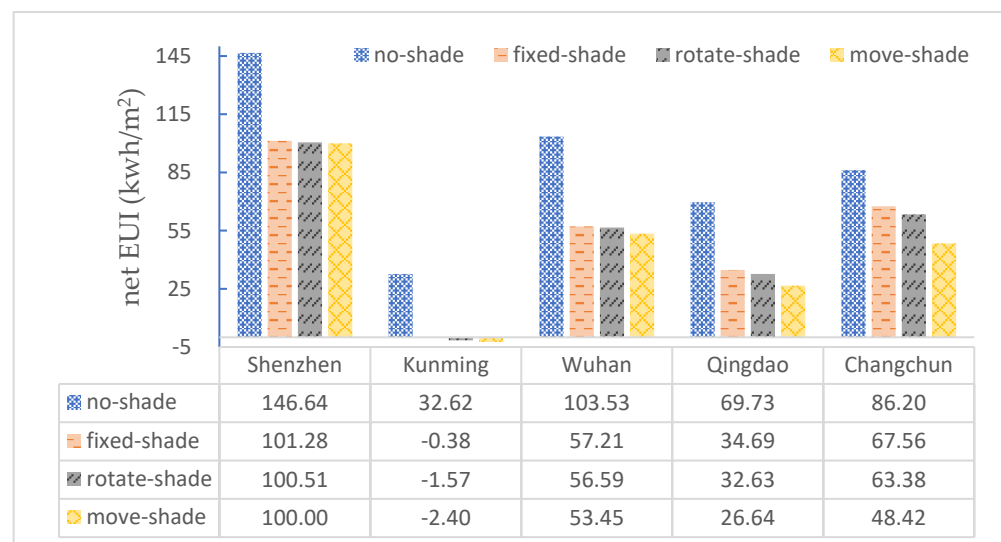


**Figure 12.** The annual net EUI by using different PVSD Strategies in the five case-study cities.

In order to understand the economic feasibility of the three PVSD strategies in different cities, the economic benefits of fixed-shade, rotate-shade, and move-shade strategies are calculated in terms of the payback period, which refers to the amount of time that a certain activity takes to recover the cost of an investment. The longer the payback period is, the lower is the economic feasibility of the activity. The calculation formula for the payback period of the PVSD is to divide the initial investment by the annual cash inflow, as shown in the formula (2) [42]:

$$\text{Payback Period (PP)} = \frac{\text{Initial Investment}}{\text{Cash inflow per year}} \quad (2)$$

The initial investment was 3686 yuan, which included the costs of the battery (800 yuan), electricity conversion and storage devices (2658 yuan), and external mechanical devices (228 yuan). Many photovoltaic manufacturers provide 25 years of warranty, so this study assumes that the service time of the PVSD was 25 years with no maintenance costs. Table 2

shows the lowest electricity price of each city according to the national electricity price list [43].

**Table 2.** The lowest electricity price in five case study cities.

Residential Electricity	Shenzhen	Kunming	Wuhan	Qingdao	Changchun
Price (yuan)/kWh	0.68	0.42	0.56	0.55	0.53

The payback period of each city is indicated in Figure 13. The payback period was the shortest in Shenzhen by using the three PVSD strategies. When adopting the fixed-shade and rotate-shade strategies, the payback period was the longest in Changchun. However, the payback period was the longest in Kunming when using the move-shade strategy. Although Kunming can achieve net-zero energy consumption by using the three strategies, the payback period can still be as long as six years. This is mainly because of the low electricity price in Kunming. The payback period of using the fixed-shade strategy of the PVSD in Changchun can be as long as 16.45 years, but the time can be shortened in half when adopting the move-shade strategy. When using the fixed PVSD in Qingdao, the payback period was 8.43 years, whereas the time can be shortened by 1.57 years if the move-shade PVSD strategy was adopted. Therefore, assuming the electricity price was stable and there was no maintenance cost, it was economically feasible to install PVSD on student apartments in China.

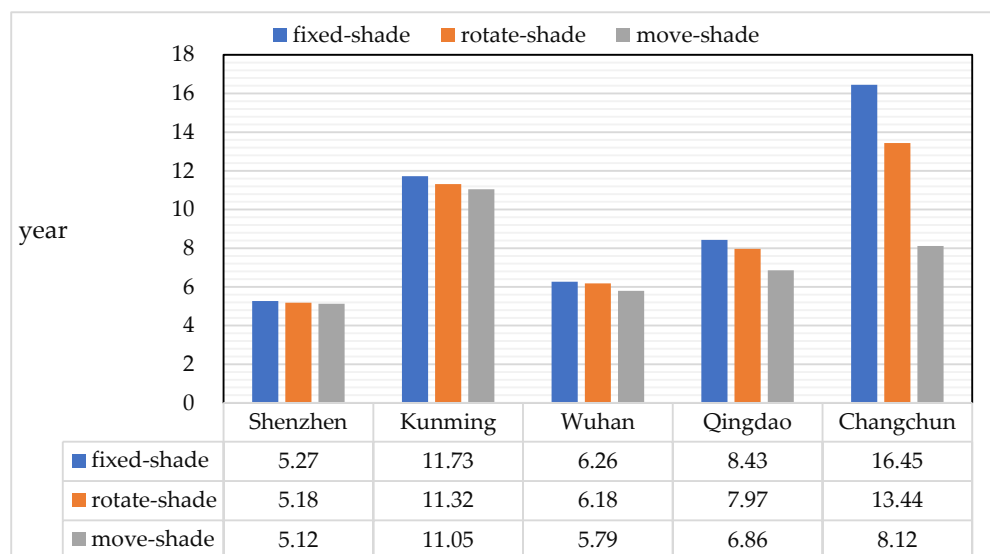


**Figure 13.** Payback period of different PVSD Strategies in the five case-study cities.

#### 4. Discussion

In order to evaluate the performance of three different types of PVSD design strategies (fixed-shade, rotate-shade, and move-shade), the optimal tilt angles and heights for different strategies were calculated through the proposed simulation program, which was created based on the parametric performance method. The electricity generation, energy consumption, and the payback period of each PVSD strategy in five Chinese cities were analyzed and compared. Existing studies indicate that there are many parameters that can affect the results. The inclination angles could be rather different for each case study due to the complexity and interrelationship between the various parameters [5]. For example, Zhang et al. found that 30° was the optimal angle for electricity generation in an office building in Hongkong, but the optimal angle could be changed to 20° if the cooling load was taken into consideration [31]. Paydar [29] studied the PVSD in a flat in Tehran, and in-

indicated that when the height was 0 m, the optimal angle was 40° to generate the maximum amount of electricity; but when the height was 0.5 m, the angle was changed to 35°. In this study, the optimal angles and heights were calculated according to the lowest amount of net energy use intensity (the difference between energy consumption and production). Each PVSD strategy and its related results were discussed in Section 3.3.

Due to the complexity of the application of PVSD on buildings, the major limitation of the study is that these results which were generated from the simulation in student apartments in China can only provide useful suggestions for the PVSD application in student apartments in China. For office and residential buildings, similar studies using the proposed simulation program will be further studied to understand the performance of PVSD applications in the future. Moreover, actual experiments can be carried out in different cities in China to see how different PVSD strategies perform in reality under the influence of various factors. More PVSD strategies can be tested and evaluated when multiple targets (for instance, daylight, energy consumption, and thermal comfort) need to be met.

In summary, there are many parameters involved in the evaluation of the PVSD energy performance. These parameters can influence the net energy consumption and have rather complicated relationships with each other. Applying an appropriate strategy to PVSD requires systematic simulation and analysis according to the specific condition of the study subject. This study proposes a parametric performance design method to simplify PVSD building simulation process to resolve complicated multiple objective evaluations. It provides an all-in-one program for non-professionals to evaluate PVSD energy consumption through simulation in just one click. It is found that adopting PVSD on building facades can effectively reduce energy consumption. A more dynamic PVSD system can generate a more energy-efficient solution. That is to say, dynamic PVSD should be considered in the design and renovation of building facades in China.

## 5. Conclusions

This research simulated the application of three PVSD strategies (fixed-shade, rotate-shade, and move-shade) in student apartments by using the proposed parametric performance design method. These strategies were used in five Chinese cities located in different climate zones. The influence of each strategy on the annual net energy use intensity of a room in the middle of a student apartment was analyzed and discussed. The optimization of the PVSD system in this study was built on the energy-consumption simulation tools of Ladybug and Honeybee on the Grasshopper platform that can simplify the simulation process.

Overall, the results indicated that applying the PVSD in building design and reconstruction can effectively reduce the overall energy consumption, mainly reducing the amount of energy used for cooling. The move-shade strategy can provide the best energy-saving performance, followed by rotate-shade and fixed-shade strategies. In summer, it was better to set the PVSD to a smaller angle and to not move it on the facade. For cities with strong heating demand in winter, it was better to move the PVSD while keeping them to larger tilt angles (more than 50°). Furthermore, the results indicated that Kunming achieved net-zero energy consumption. Compared to the no-shade strategy, the reduction of the net EUI by using the move-shade strategy was 31.80% in Shenzhen, 48.37% in Wuhan, 61.79% in Qingdao, and 43.83% in Changchun. In areas with huge heating demand, using the PVSD may even cause an increase in energy consumption. Various types of climates and electricity prices can affect the efficiency and economic payback period of the PVSD application, but the PVSD can still provide a generally positive effect for all cities in China. Under the premise that the maintenance cost was not considered, the payback period ranged between 5 to 16 years when using PVSD in different climate zones. Among them, the payback periods of rotate and move-shade strategies were shorter than that of the fixed-shade strategies, and the payback can be achieved 1–8 years in advance. It is recommended

to use fixed-shade strategy in Shenzhen and Kunming, and to adopt move-shade strategy in Wuhan, Qingdao, and Changchun.

**Author Contributions:** Conceptualization, Q.M. and X.W.; methodology, Q.M.; software, Q.M. and W.L.; validation, W.L.; writing—original draft preparation, X.C. and Q.M.; writing—review and editing, X.C. and Q.M.; visualization, W.L. and Q.X.; funding acquisition, Q.M. All authors have read and agreed to the published version of the manuscript.

**Funding:** This research is supported by grants from the National Natural Science Foundation of China (No. 52108015) and the Natural Science Foundation of Shandong Province (No. ZR201910280141).

**Data Availability Statement:** The data presented in this study are available on request from the corresponding author. The data are not publicly available due to relevant data protection laws.

**Acknowledgments:** We would like to express our gratitude to the editors and reviewers for their thoughtful comments and constructive suggestions on improving the quality of the paper.

**Conflicts of Interest:** The authors declare no conflict of interest.

## References

1. Building on the Past, Starting a New Journey to Address Climate Change Globally. Available online: [http://www.gov.cn/gongbao/2020/issue\\_8786.htm](http://www.gov.cn/gongbao/2020/issue_8786.htm) (accessed on 12 December 2020).
2. Notice of the State Council on the Issuance of the Action Plan for Carbon Peaking by 2030. Available online: [http://www.gov.cn/gongbao/2021/issue\\_9406.htm](http://www.gov.cn/gongbao/2021/issue_9406.htm) (accessed on 24 October 2021).
3. Che, X.-J.; Zhou, P.; Chai, K.-H. Regional policy effect on photovoltaic (PV) technology innovation: Findings from 260 cities in China. *Energy Policy* **2022**, *162*, 112807. [[CrossRef](#)]
4. Hao, D.; Qi, L.; Tairab, A.M.; Ahmed, A.; Azam, A.; Luo, D.; Pan, Y.; Zhang, Z.; Yan, J. Solar energy harvesting technologies for PV self-powered applications: A comprehensive review. *Renew. Energy* **2022**, *188*, 678–697. [[CrossRef](#)]
5. Kirmat, A.; Tasgetiren, M.F.; Brida, P.; Krejcar, O. Control of PV integrated shading devices in buildings: A review. *Build. Environ.* **2022**, *214*, 108961. [[CrossRef](#)]
6. Florio, P.; Peronato, G.; Perera, A.T.D.; Di Blasi, A.; Poon, K.H.; Kämpf, J.H. Designing and assessing solar energy neighborhoods from visual impact. *Sustain. Cities Soc.* **2021**, *71*, 102959. [[CrossRef](#)]
7. Scognamiglio, A. A Trans-Disciplinary Vocabulary for Assessing the Visual Performance of BIPV. *Sustainability* **2021**, *13*, 5500. [[CrossRef](#)]
8. Aguacil, S.; Lufkin, S.; Rey, E. Active surfaces selection method for building-integrated photovoltaics (BIPV) in renovation projects based on self-consumption and self-sufficiency. *Energy Build.* **2019**, *193*, 15–28. [[CrossRef](#)]
9. Al-Masrani, S.M.; Al-Obaidi, K.M. Dynamic shading systems: A review of design parameters, platforms and evaluation strategies. *Autom. Constr.* **2019**, *102*, 195–216. [[CrossRef](#)]
10. Singh, B.P.; Goyal, S.K.; Siddiqui, S.A. Analysis and Classification of Maximum Power Point Tracking (MPPT) Techniques: A Review. In *Intelligent Computing Techniques for Smart Energy Systems—Proceedings of ICTSES 2018*; Springer: Singapore, 2020; pp. 999–1008.
11. Boito, P.; Grena, R. Application of a fixed-receiver Linear Fresnel Reflector in concentrating photovoltaics. *Sol. Energy* **2021**, *215*, 198–205. [[CrossRef](#)]
12. Gupta, M.; Dubey, A.K.; Kumar, V.; Mehta, D.S. Experimental study of combined transparent solar panel and large Fresnel lens concentrator based hybrid PV/thermal sunlight harvesting system. *Energy Sustain. Dev.* **2021**, *63*, 33–40. [[CrossRef](#)]
13. Agyekum, E.B.; PraveenKumar, S.; Alwan, N.T.; Velkin, V.I.; Shcheklein, S.E. Effect of dual surface cooling of solar photovoltaic panel on the efficiency of the module: Experimental investigation. *Heliyon* **2021**, *7*, e07920. [[CrossRef](#)]
14. Agyekum, E.B.; PraveenKumar, S.; Alwan, N.T.; Velkin, V.I.; Adebayo, T.S. Experimental Study on Performance Enhancement of a Photovoltaic Module Using a Combination of Phase Change Material and Aluminum Fins—Exergy, Energy and Economic (3E) Analysis. *Inventions* **2021**, *6*, 69. [[CrossRef](#)]
15. Agyekum, E.B.; PraveenKumar, S.; Alwan, N.T.; Velkin, V.I.; Shcheklein, S.E.; Yaqoob, S.J. Experimental Investigation of the Effect of a Combination of Active and Passive Cooling Mechanism on the Thermal Characteristics and Efficiency of Solar PV Module. *Inventions* **2021**, *6*, 63. [[CrossRef](#)]
16. PraveenKumar, S.; Agyekum, E.B.; Velkin, V.I.; Yaqoob, S.J.; Adebayo, T.S. Thermal management of solar photovoltaic module to enhance output performance: An experimental passive cooling approach using discontinuous aluminum heat sink. *Int. J. Renew. Energy Res.* **2021**, *11*, 1700–1712.
17. De Vries, S.B.; Loonen, R.C.G.M.; Hensen, J.L.M. Simulation-aided development of automated solar shading control strategies using performance mapping and statistical classification. *J. Build. Perform. Simul.* **2021**, *14*, 770–792. [[CrossRef](#)]
18. Taveres-Cachat, E.; Lobaccaro, G.; Goia, F.; Chaudhary, G. A methodology to improve the performance of PV integrated shading devices using multi-objective optimization. *Appl. Energy* **2019**, *247*, 731–744. [[CrossRef](#)]

19. Hofer, J.; Groenewolt, A.; Jayathissa, P.; Nagy, Z.; Schlueter, A. Parametric analysis and systems design of dynamic photovoltaic shading modules. *Energy Sci. Eng.* **2016**, *4*, 134–152. [[CrossRef](#)]
20. Kosorić, V.; Lau, S.-K.; Tablada, A.; Bieri, M.; Nobre, A.M. A Holistic Strategy for Successful Photovoltaic (PV) Implementation into Singapore's Built Environment. *Sustainability* **2021**, *13*, 6452. [[CrossRef](#)]
21. Yang, R.J.; Zou, P.X.W. Building integrated photovoltaics (BIPV): Costs, benefits, risks, barriers and improvement strategy. *Int. J. Constr. Manag.* **2015**, *16*, 39–53. [[CrossRef](#)]
22. Mofidi, F.; Akbari, H. Intelligent buildings: An overview. *Energy Build.* **2020**, *223*, 110192. [[CrossRef](#)]
23. Lufkin, S. Towards dynamic active façades. *Nat. Energy* **2019**, *4*, 635–636. [[CrossRef](#)]
24. Svetozarevic, B.; Begle, M.; Jayathissa, P.; Caranovic, S.; Shepherd, R.F.; Nagy, Z.; Hischer, I.; Hofer, J.; Schlueter, A. Dynamic photovoltaic building envelopes for adaptive energy and comfort management. *Nat. Energy* **2019**, *4*, 671–682. [[CrossRef](#)]
25. Ramadan, A.; Kamel, S.; Hamdan, I.; Agwa, A.M. A Novel Intelligent ANFIS for the Dynamic Model of Photovoltaic Systems. *Mathematics* **2022**, *10*, 1286. [[CrossRef](#)]
26. Kirmat, A.; Krejcar, O.; Ekici, B.; Fatih Tasgetiren, M. Multi-objective energy and daylight optimization of amorphous shading devices in buildings. *Sol. Energy* **2019**, *185*, 100–111. [[CrossRef](#)]
27. Ridha, H.M.; Gomes, C.; Hizam, H.; Ahmadipour, M.; Heidari, A.A.; Chen, H. Multi-objective optimization and multi-criteria decision-making methods for optimal design of standalone photovoltaic system: A comprehensive review. *Renew. Sustain. Energy Rev.* **2021**, *135*, 110202. [[CrossRef](#)]
28. Fouad, M.M.; Shihata, L.A.; Morgan, E.I. An integrated review of factors influencing the performance of photovoltaic panels. *Renew. Sustain. Energy Rev.* **2017**, *80*, 1499–1511. [[CrossRef](#)]
29. Akbari Paydar, M. Optimum design of building integrated PV module as a movable shading device. *Sustain. Cities Soc.* **2020**, *62*, 102368. [[CrossRef](#)]
30. Krarti, M. Evaluation of PV integrated sliding-rotating overhangs for US apartment buildings. *Appl. Energy* **2021**, *293*, 116942. [[CrossRef](#)]
31. Zhang, W.L.; Lu, L.; Peng, J.Q. Evaluation of potential benefits of solar photovoltaic shadings in Hong Kong. *Energy* **2017**, *137*, 1152–1158. [[CrossRef](#)]
32. Sun, C.; Liu, Q.; Han, Y. Many-Objective Optimization Design of a Public Building for Energy, Daylighting and Cost Performance Improvement. *Appl. Sci.* **2020**, *10*, 2435. [[CrossRef](#)]
33. Ladybug Tools, Food4rhino Apps for Rhino and Grasshopper. Available online: <https://www.food4rhino.com/en/app/ladybug-tools> (accessed on 11 January 2022).
34. Barzegar Ganji, H.; Utzinger, D.M.; Bradley, D.E. Create and Validate Hybrid Ventilation Components in Simulation Using Grasshopper and Python in Rhinoceros. In Proceedings of the 16th IBPSA International Conference and Exhibition, Rome, Italy, 2–4 September 2019; pp. 4345–4352.
35. Feng, K.; Lu, W.; Wang, Y. Assessing environmental performance in early building design stage: An integrated parametric design and machine learning method. *Sustain. Cities Soc.* **2019**, *50*, 101596. [[CrossRef](#)]
36. De Sousa Freitas, J.; Cronemberger, J.; Soares, R.M.; Amorim, C.N.D. Modeling and assessing BIPV envelopes using parametric Rhinoceros plugins Grasshopper and Ladybug. *Renew. Energy* **2020**, *160*, 1468–1479. [[CrossRef](#)]
37. EnergyPlus™ Version 22.1.0 Documentation Application Guide for EMS. Available online: [https://energyplus.net/assets/nrel\\_custom/pdfs/pdfs\\_v22.1.0/EMSApplicationGuide.pdf](https://energyplus.net/assets/nrel_custom/pdfs/pdfs_v22.1.0/EMSApplicationGuide.pdf) (accessed on 29 March 2022).
38. General Code for Energy Efficiency and Renewable Energy Application in Buildings GB 55015-2021. Available online: <http://www.jianbiaoku.com/webarbs/book/160785/4633673.shtml> (accessed on 1 April 2022).
39. BIPRO TD7G66M 10BB 132 Half-Cell. Available online: <https://www.talesun.com/en/download/num/> (accessed on 29 March 2022).
40. Climate.OneBuilding.Org. Available online: <https://climate.onebuilding.org/default.html> (accessed on 24 April 2022).
41. Building Climate Zoning Standards GB 50178-93. Available online: <http://www.jianbiaoku.com/webarbs/book/12519/2916745.shtml> (accessed on 1 February 1994).
42. Zeraatpisheh, M.; Arababadi, R.; Saffari Pour, M. Economic Analysis for Residential Solar PV Systems Based on Different Demand Charge Tariffs. *Energies* **2018**, *11*, 3271. [[CrossRef](#)]
43. State Grid Corporation of China. Available online: <http://www.sgcc.com.cn/> (accessed on 29 March 2022).